Global variational quantum circuits for arbitrary symmetric state preparation

Liam J. Bond [1,2,3,*] Matthew J. Davis,[3] Jiří Minář [1,2,4] Rene Gerritsma [1,2]
Gavin K. Brennen [5] and Arghavan Safavi-Naini[1,2,3]

[1]*Institute of Physics, University of Amsterdam, Science Park 904, 1098 XH Amsterdam, the Netherlands*
[2]*QuSoft, Science Park 123, 1098 XG Amsterdam, the Netherlands*
[3]*ARC Centre of Excellence for Engineered Quantum Systems, School of Mathematics and Physics,*
University of Queensland, St Lucia, QLD 4072, Australia
[4]*CWI, Science Park 904, 1098 XH Amsterdam, the Netherlands*
[5]*ARC Centre of Excellence for Engineered Quantum Systems, School of Mathematical and Physical Sciences,*
Macquarie University, Sydney, NSW 2109, Australia

Quantum states that are symmetric under particle exchange play a crucial role in fields such as quantum metrology and quantum error correction. We use a variational circuit composed of global one-axis twisting and global rotations to efficiently prepare arbitrary symmetric states, i.e., any superposition of Dicke states. The circuit does not require local addressability or ancilla qubits and thus can be readily implemented in a variety of experimental platforms including trapped-ion quantum simulators and cavity QED systems. We provide analytic and numerical evidence that any N-qubit symmetric state can be prepared in $2N/3$ steps. We demonstrate the utility of our protocol by preparing (i) metrologically useful N-qubit Dicke states of up to $N = 300$ qubits in $\mathcal{O}(1)$ gate steps with theoretical infidelities $1 - \mathcal{F} < 10^{-3}$, (ii) the $N = 9$ Ruskai codewords in $P = 4$ gate steps with $1 - \mathcal{F} < 10^{-4}$, and (iii) the $N = 13$ Gross codewords in $P = 7$ gate steps with $1 - \mathcal{F} < 10^{-4}$. Focusing on trapped-ion platforms, for the $N = 9$ Ruskai and $N = 13$ Gross codewords we estimate that the protocol achieves fidelities $\gtrsim 95\%$ in the presence of typical experimental noise levels, thus providing a pathway to the preparation of a wide range of useful highly entangled quantum states.

Introduction. The operation of a quantum computer relies on our ability to prepare highly entangled quantum states, both as a step for quantum algorithms, and as codewords for quantum error correction (QEC). Despite recent remarkable experimental progress toward fault-tolerant quantum computing [1–3], the fragility of multipartite entanglement to noise limits the fidelity of state preparation. Furthermore, the lack of single-site addressing in some experimental platforms has typically limited the variety of states that can be prepared to, e.g., squeezed states. In light of these limitations, the choice of QEC scheme is important. Depending on its properties, certain QEC schemes may offer advantages both in terms of the types of errors that they can protect against [4], as well as their suitability of implementation to the particular hardware. One promising approach utilizes codewords which are symmetric states, i.e., superpositions of Dicke states [5–7]. The Dicke states are also relevant for quantum metrology [8], including error-corrected quantum sensing [9], quantum storage [10,11], and quantum networking [12]. The need to overcome the intrinsic noise in NISQ devices has motivated the design of symmetric state preparation protocols that minimize the circuit depth. In particular, symmetric states have been prepared using one- and two-qubit gate circuits with depth $\mathcal{O}(N)$ [13,14], and specific Dicke states with constant depth using measurements and classical computation [15].

In this article, we demonstrate that arbitrary superpositions of Dicke states can be engineered using linear depth circuits with only global control. Specifically, we utilize a variational quantum circuit consisting of only global one-axis twisting and global rotations, and thus do not demand local addressability nor ancilla qubits. We provide analytic and numerical evidence that the number of steps to synthesize an arbitrary N-qubit symmetric state scales as $2N/3$. Focusing on applications to QEC codewords, we show that only $P = 4$ and $P = 7$ steps are required to prepare QEC codewords of the $N = 9$ Ruskai [6] and $N = 13$ Gross [7] codes with infidelity $1 - \mathcal{F} < 10^{-4}$, respectively. We discuss the possible implementation in trapped ions, including a detailed analysis of expected sources of error. The limited resources required by our protocol make it immediately realizable on a broad range of experimental quantum simulation platforms.

Dicke states. We consider an ensemble of N qubits. The collective spin operators are defined as $J_\alpha = (1/2) \sum_{j=1}^{N} \sigma_j^\alpha$ where $\alpha \in \{x, y, z\}$ and σ_j^α is the Pauli operator acting on the jth qubit. Dicke states, denoted $|J, M\rangle$, are simultaneous eigenstates of the total spin operator $J^2 = J_x^2 + J_y^2 + J_z^2$ and
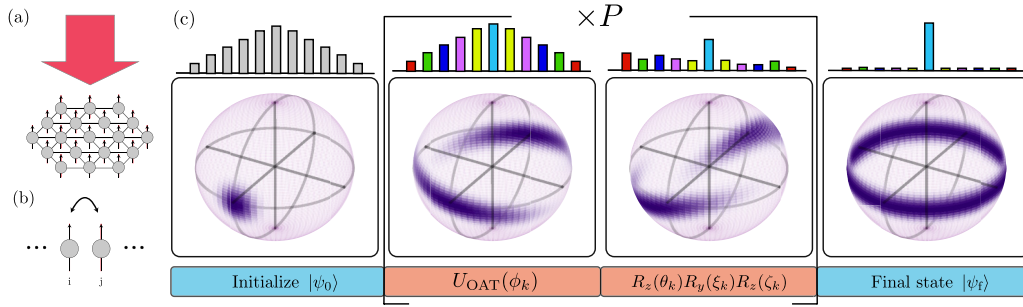
*Contact author: L.J.Bond@uva.nl

FIG. 1. (a) The protocol Eq. (2) utilizes operations that act globally on a collection of N qubits. (b) The Dicke states are symmetric, i.e., any two qubits i and j can be interchanged without changing the quantum state. (c) Schematic representation of the protocol. The system is initialized in a coherent spin state (CSS) $|\psi_0\rangle = |\bar{\theta}, \bar{\phi}\rangle$. Next, one-axis twisting U_{OAT} generates spin squeezing. For relatively small ϕ_k the CSS is spin squeezed; for larger ϕ_k the probability distribution separates across the Bloch sphere, as is the case sketched here. Next, the state is rotated about an arbitrary axis. These two operations are repeated P times, with parameters numerically optimized to minimize the infidelity $1 - \mathcal{F}$. Above the Bloch spheres, to highlight the connection to amplitude amplification, we sketch the $N + 1$ basis state amplitudes with coloring representing complex phase. In this perspective, U_{OAT} applies a phase that depends nonlinearly on the excitation number M, with the rotation then amplifying or attenuating the amplitude conditioned on the phase that was applied. Repeated application of U_{OAT} and R with optimized parameters can therefore maximize the amplitude of a target state.

J_z. The quantum numbers J and M are defined by $J^2|J, M\rangle = J(J + 1)|J, M\rangle$, $J_z|J, M\rangle = M|J, M\rangle$ with $J \in \{0, \ldots, N/2\}$, and $M \in \{-J, \ldots, J\}$. We focus on the $N + 1$ symmetric $J \equiv N/2$ Dicke states, which in the single-particle σ_z basis are

$$|J = N/2, M\rangle = \frac{1}{\sqrt{\lambda}} \sum_{\mathcal{P}} (|1\rangle^{J+M} \otimes |0\rangle^{J-M}), \qquad (1)$$

where the normalization factor is $\lambda = \binom{2J}{J+M}$, and where the summation is over all permutations $\mathcal{P}$ of the ordering of the spins [16]. Dicke states feature entanglement that is persistent [17] and robust to particle loss [18–20] which makes them attractive for experimental realization, while also demonstrating useful sensing capabilities [21,22]. Specifically, the N-qubit W-state $|N/2, -N/2 + 1\rangle$ is maximally pairwise entangled [23,24], while the Dicke state with $N/2$ excitations $|N/2, 0\rangle$ saturates the quantum Cramér-Rao bound when sensing global rotations about the x-y axis [25]. There are many existing deterministic preparation protocols for Dicke states, including quantum circuit approaches that use one- and two-qubit gates [13–15], global pulse schemes [25–28], and others [29–31].

In addition to bare Dicke states, superpositions of Dicke states are of key interest. For example, the Greenberger–Horne–Zeilinger (GHZ) state $|\mathrm{GHZ}\rangle = |N/2, -N/2\rangle + |N/2, N/2\rangle$ is maximally entangled, represents a distinct class of multipartite entanglement, exhibits phase sensing sensitivity below the standard quantum limit (SQL) [32,33], and has been prepared in many experimental platforms [34–36]. More generally, superpositions over more of the Dicke states form the logical basis states of various QEC codes including Pauli exchange error correcting codes [6] and large spin codes [7]. The weighting of individual Dicke states in each of these logical basis states are chosen to satisfy the Knill-Laflamme QEC conditions [37]. Existing protocols to prepare such specific, highly entangled superpositions of Dicke states typically require single-site addressability [38] or a large detuning limit [39]. Below, we alleviate these constraints and propose to prepare Dicke state superpositions using a global variational quantum circuit.

State preparation protocol. Global variational quantum circuits have been previously proposed [40–43] and demonstrated experimentally [44] for the preparation of squeezed quantum states for quantum metrology. Here, instead of optimizing the variational parameters to maximize a property of the target state (such as the squeezing amplitude or phase sensitivity), we employ such circuits to prepare target symmetric quantum states by minimizing the infidelity $1 - \mathcal{F} = 1 - |\langle \psi_t | \psi_f \rangle|^2$, where $|\psi_t\rangle$ is a chosen target state, $|\psi_f\rangle = U_{\mathrm{tot}}|\psi_0\rangle$ the final state, and $|\psi_0\rangle$ the initial state. As sketched in Fig. 1, the circuit of P layers is

$$U_{\mathrm{tot}} = \prod_{k=1}^{P} [R(\theta_k, \xi_k) U_{\mathrm{OAT}}(\phi_k)], \qquad (2)$$

and consists of (i) global rotations $R(\theta_k, \xi_k) = R_z(\theta_k) R_y(\xi_k)$, and (ii) global one-axis twisting $U_{\mathrm{OAT}}(\phi) = e^{i\phi J_z^2}$, where $\phi = gt$ with g the coupling strength and t the evolution time [45]. Because R_z commutes with U_{OAT}, for $P \geqslant 2$ the global rotation R is about an arbitrary axis. Although the fidelity can be efficiently computed classically because the symmetric space dimension is $N + 1$, in the Supplemental Material we discuss how an upper bound on the infidelity can be efficiently computed on quantum devices for a hybrid classical-quantum algorithm approach, which may be a preferred option to mitigate certain hardware errors [46].

The capability of the protocol to prepare superpositions of Dicke states can be understood using amplitude amplification, as sketched in Fig. 1. To emphasize the versatility of the variational circuit, we note that U_{OAT} and R provide universal control over the symmetric subspace [43,47]. Although a general explicit expression for the optimal parameters for arbitrary symmetric state synthesis is a complicated task, a simple consistency argument for the minimum number of gates P^* to prepare a general symmetric state can be made as follows: accounting for the coefficients and normalization of the $N + 1$ basis states, a general state in the symmetric
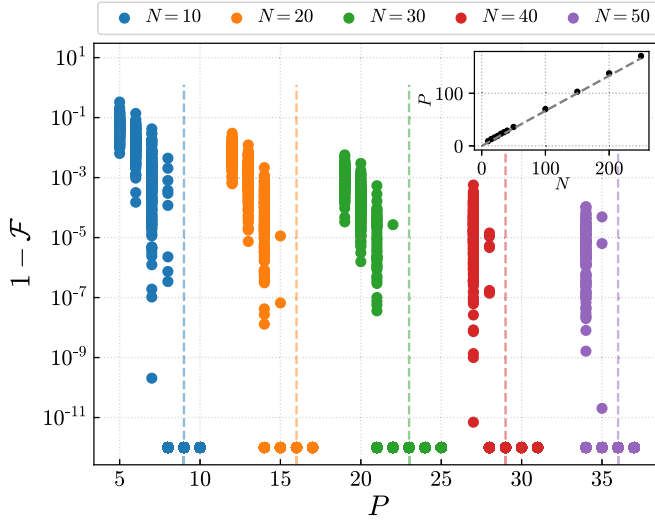
FIG. 2. Infidelity $1 - \mathcal{F} = 1 - |\langle\psi_{\mathrm{t}}|\psi_{\mathrm{f}}\rangle|^2$ vs circuit depth P for various N. Each data point is a Haar random target state; we draw $N_{\mathrm{Haar}} = 200$ targets for each N. The variational parameters are classically optimized using a local optimization algorithm. As the system becomes controllable, all local minima become global minima, which corresponds for each N to the sharp decrease in infidelity as P increases (marked with vertical dashed lines). Inset: location of the transition as a function of N (black points) for up to $N = 250$, demonstrating excellent agreement with the scaling prediction $P^* = 2N/3$ (gray dashed).

FIG. 3. (a) Theoretical infidelity $1 - \mathcal{F} = 1 - |\langle\psi_{\mathrm{t}}|\psi_{\mathrm{f}}\rangle|^2$ to prepare: the the W state $|N/2, -N/2 + 1\rangle$ (solid blue) and $N/2$ excitation state $|N/2, 0\rangle$ (dashed orange) using the protocol U_{tot} Eq. (2) for $P = 2$ (dots), $P = 3$ (diamonds), and $P = 4$ (squares). The lines show a power law fit, with excellent agreement. Both target states can be prepared with small theoretical infidelities $1 - \mathcal{F} < 10^{-3}$ in $P = 3$ and $P = 4$ gate steps, respectively, in systems as large as $N = 300$ qubits. (b) The su(2) Husimi Q representation for the $P = 3$ solution that prepares $|N/2, 0\rangle$ with $N = 300$. The optimized initial coherent spin state starts along x, with the subsequent interleaving of one-axis twisting and global rotations leading to the preparation of $|\psi_t\rangle$ with $1 - \mathcal{F} \sim 10^{-2}$.

$J = N/2$ subspace is described by $2N$ real parameters. As each protocol step is characterized by three free parameters θ, ξ, ϕ, the preparation of an arbitrary symmetric state requires $P^* = 2N/3$ steps.

We numerically verify the scaling relation for P^* by generating $N_{\mathrm{Haar}} = 200$ Haar random states as target states and optimizing the protocol's variational parameters to minimize $1 - \mathcal{F}$. Obtaining (and verifying) a global minima is challenging, as in general the optimization landscape can contain many local minima. However, if the system is controllable [48], then every local minima is a global minima [49]. As such, performing only local optimization of the parameters, we expect a sharp transition in target state infidelity at some $P \geqslant P^*$ as the system becomes controllable.

In Fig. 2 we plot the infidelity $1 - \mathcal{F}$ as a function of P for various N up to $N = 50$. We perform local gradient-based optimization using BFGS [50] in JULIA [51] with OPTIM.JL and LINESEARCHES.JL [52], and terminate the optimization once the infidelity passes below a threshold $\epsilon = 10^{-12}$. As expected, as P increases the infidelity decreases, with a relatively sharp transition as the system becomes controllable. In the inset of Fig. 2 we plot the location of the transition as a function of N, showing excellent agreement with the scaling obtained from counting, $P^* = 2N/3$. As shown in the inset we further verify this prediction by optimizing the parameters for $N_{\mathrm{Haar}} = 200$ Haar random states using $P = \lceil 2N/3 \rceil + c$ gates with a small constant offset c [53] for $N = 100$, $N = 150$, $N = 200$, and $N = 250$, verifying that all states can be prepared with infidelities below the optimization termination threshold $\epsilon = 10^{-12}$. Therefore the protocol Eq. (2) is an efficient preparation protocol for synthesizing arbitrary sym-
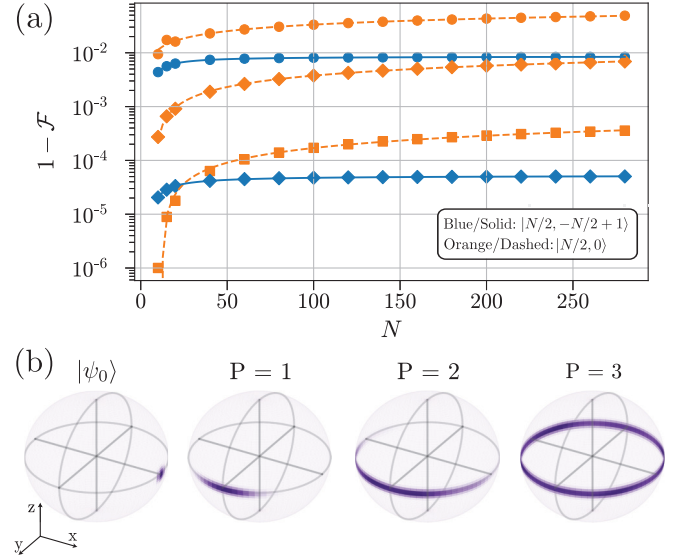
metric states. To the best of our knowledge this improves upon previous global control protocols, which required N steps only in a large detuning limit [39] or using excited Rydberg states [54], and $\mathcal{O}(N^4)$ steps for arbitrary unitary synthesis [43].

Dicke state preparation. Next, we demonstrate the preparation of specific states, beginning with bare Dicke states. Because the gate sequence Eq. (2) starts with the application of U_{OAT}, for the initial state we choose a global rotation acting on $|N/2, -N/2\rangle$, which is a coherent spin state (CSS) $|\psi_0\rangle = |\bar{\theta}, \bar{\phi}\rangle$, i.e., an eigenstate of the spin component in the $(\bar{\theta}, \bar{\phi})$ direction. The parameters $(\bar{\theta}, \bar{\phi})$ are also numerically optimized, and thus the total number of free parameters is $3P + 2$. Both here and in the next section, the numerical optimization uses a multistart Monte Carlo search, with local optimization using L-BFGS [55].

First, we prepare the Dicke state with $N/2$ excitations, $|\psi_{\mathrm{t}}\rangle = |N/2, 0\rangle$. This state is metrologically useful: when the state used for sensing is $|N/2, 0\rangle$, the uncertainty in the measured angle ϵ of a rotation $e^{-i\epsilon J_y}$ saturates the Cramer-Rao bound, $(\Delta\epsilon)^2 = 2/[N(N + 2)]$ and features entanglement that is robust to particle loss [18–20,56,57]. In Fig. 3(a) we plot (dashed orange) $1 - \mathcal{F}$ as a function of N for $P = 2$ (circles), $P = 3$ (diamonds), and $P = 4$ (squares). The infidelity is remarkably robust to increasing qubit number, with $P = 4$ gates sufficient to prepare the target state in up to $N = 300$ qubits with $1 - \mathcal{F} \lesssim 10^{-3}$. The dashed lines show a power law fit with excellent agreement, emphasizing the slow increase of

infidelity with N for $N \gtrsim 50$. In Fig. 3(b) we plot the evolution of the $N = 300$ state under the $P = 3$ gate sequence solution using the su(2) Husimi Q representation $Q(\theta, \phi) = \langle \theta, \phi | \rho | \theta, \phi \rangle$ of a state ρ where $| \theta, \phi \rangle$ is a CSS. Clearly visible is the effect of spin squeezing, whose repeated application combined with global rotations results in the preparation of $|N/2, 0\rangle$.

Second, we prepare the N-qubit W state, $|N/2, -N/2 + 1\rangle$. In Fig. 3(a), we plot (solid blue) the infidelity to prepare the W state with $P = 2$ (circles) and $P = 3$ (diamonds) [58]. We find that the W state can be prepared in systems of up to $N = 300$ qubits with small infidelities $1 - \mathcal{F} < 10^{-4}$ in only $P = 3$. Thus, our protocol can be used to prepare these two Dicke states in up to $N = 300$ qubits in $\mathcal{O}(1)$ gate steps.

Quantum error correction codewords. Next, we prepare specific superpositions of Dicke states for QEC. Pauli exchange errors are two-qubit errors that arise due to interactions between qubits, for example due to dipole-dipole interactions. Physically, exchange errors are similar to bit flip errors, with the additional constraint that a qubit will flip if and only if its neighbor is different. Codes such as the nine-qubit Shor code [59] cannot distinguish between exchange errors and phase errors. The Ruskai code [6] exploits the permutation invariance of Dicke states to correct all one-qubit errors and Pauli exchange errors. The explicit codewords for $N = 9$ are

$$|R_0\rangle = |9/2, -9/2\rangle/2 + \sqrt{3/4}|9/2, 3/2\rangle, \qquad (3a)$$

$$|R_1\rangle = |9/2, 9/2\rangle/2 + \sqrt{3/4}|9/2, -3/2\rangle. \qquad (3b)$$

As a second example, we consider the Gross codes [7]. Designed such that the logical single-qubit Clifford operations are global rotations, the Gross code is immune, to first order, to errors that correspond to global rotations. As such, the code utilizes interactions that are native to many experimental platforms, and protects against the typically most deleterious sources of noise, including both T_1-type relaxation and T_2-type dephasing errors. The smallest collective spin for which this code can be constructed is $N = 13$. It utilizes the two following states: $|\tilde{G}_{0,1}\rangle = c_1|13/2, 13/2\rangle + c_2|13/2, 5/2\rangle + c_3|13/2, -3/2\rangle + c_4|13/2, -11/2\rangle$, where the coefficients for $|\tilde{G}_0\rangle$ are $c_1 = \sqrt{910}/56$, $c_2 = -3\sqrt{154}/56$, $c_3 = -\sqrt{770}/56$, and $c_4 = \sqrt{70}/56$; and for $|\tilde{G}_1\rangle$ are $c_1 = \sqrt{231}/84$, $c_2 = \sqrt{1365}/84$, $c_3 = -\sqrt{273}/28$, and $c_4 = -\sqrt{3003}/84$. The explicit codewords are then

$$|G_0\rangle = \frac{\sqrt{105}}{14}|\tilde{G}_0\rangle + \frac{\sqrt{91}}{14}|\tilde{G}_1\rangle, \qquad (4)$$

where $|G_1\rangle$ follows from $|G_0\rangle$ by a global spin flip.

In Fig. (4) we plot the infidelity of the state $|\psi_f\rangle$ prepared using the optimized gate protocol Eq. (2) with target states $|\psi_t\rangle = |R_1\rangle$ (blue with dots) and $|\psi_t\rangle = |G_0\rangle$ (orange with stars). We find solutions that prepare the codewords with infidelities $1 - \mathcal{F} < 10^{-4}$ in only $P = 4$ and $P = 7$ gate steps, respectively. Therefore, our protocol provides a pathway toward the implementation of large N-qubit QEC codes utilizing only global addressability of the qubits constituting the codeword.

Realization in trapped ions. U_{OAT} can be realized in trapped ions by off-resonantly driving the center of mass (COM) mode [34,60–63]. Considering N ions in a linear Paul trap, two
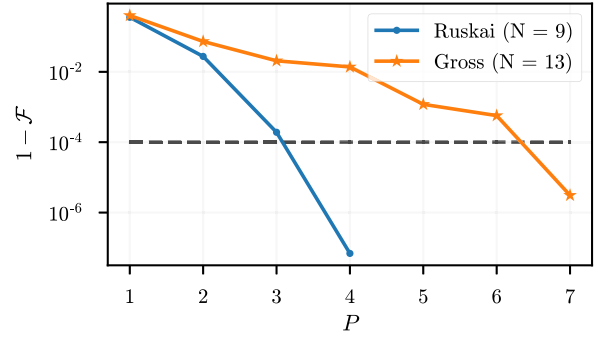

FIG. 4. Infidelity to prepare the $N = 9$ Ruskai $|R_1\rangle$ and $N = 13$ Gross $|G_0\rangle$ codewords using the optimized gate sequence as a function of P. Despite being highly specific superpositions of Dicke states, we numerically find solutions that can prepare both target states with infidelities $1 - \mathcal{F} < 10^{-4}$ in $P = 4$ and $P = 7$ gate steps for $|R_1\rangle$ and $|G_0\rangle$, respectively.

global Raman beams detuned from the red and blue sidebands by δ leads to the following Hamiltonian in the interaction picture:

$$H_I = \Omega\eta(ae^{-i\delta t} + a^\dagger e^{i\delta t})J_z, \qquad (5)$$

where we have assumed the Lamb-Dicke regime, and where a ($a^\dagger$) are the annihilation (creation) operators of the COM mode, η the Lamb-Dicke parameter, and Ω the Rabi frequency. Note that although we require the Lamb-Dicke regime, our protocol is otherwise insensitive to temperature and therefore does not require ground state cooling [60,64]. Evolving for time $t_f = 2\pi/\delta$ results in a closed loop in phase space such that the motion decouples from the spin degree of freedom. The effective evolution is described by one-axis twisting, $U_{\text{OAT}} = \exp(i\phi J_z^2)$ with $\phi = 2\pi\eta^2\Omega^2/\delta^2$ the area enclosed [65]. Our optimized solutions are typically $\phi \sim 1$. Setting $\eta\Omega = 2\pi \times 20\,\text{kHz}$ and $\delta = 2\pi \times 20\,\text{kHz}$ results in $t_f = 50\,\mu\text{s}$ and $\phi = 2\pi$. The total protocol duration T is therefore $T = Pt_f$, and thus for all the gate sequences we present $T \lesssim 350\,\mu\text{s}$.

Here we study the effects of off-resonant driving and dephasing, with laser intensity fluctuations and nonglobal beams further analyzed in the Supplemental Material [46]. Off-resonant driving of the other modes leads to nonuniform spin-dependent phases. Assuming a typical trap frequency $\omega = 2\pi \times 2\,\text{MHz}$, the stretch mode, which is the leading order correction, is detuned by $(\sqrt{3} - 1)\omega + \delta$. The area enclosed by the stretch mode is $\sim 10^{-2}$ times smaller than the area enclosed by the COM mode, and thus for realistic parameters unwanted off-resonant driving of the collective modes is negligible compared to the effects of dephasing, which we consider below.

We use a realistic dephasing rate $\gamma = 2\pi \times 5\,\text{Hz}$. The off-diagonal coherences of the GHZ state decay as $\sim e^{-\gamma N t}$, such that the fidelity can be roughly estimated as $F \sim 1/2(1 + e^{-\gamma N t})$. We assume that the rotations are noise free, as they can be performed fast relative to the spin squeezing. For the $N = 9$ Ruskai and $N = 13$ Gross protocols, using the $P = 4$ and $P = 7$ gate sequences, respectively, assuming the ideal protocol prepares the state with perfect fidelity, we estimate noisy fidelities $\mathcal{F} \sim 97\%$ and $\mathcal{F} \sim 93\%$, respectively. Reducing the

dephasing rate to $\gamma = 2\pi \times 1\text{Hz}$ increases the Ruskai and Gross codeword fidelities to $\mathcal{F} \sim 99\%$ and $\mathcal{F} \sim 98\%$, respectively. Furthermore, parametric amplification can increase the squeezing amplitude achieved in a given t_f [66], whilst multiple Raman beatnotes can reduce off-resonant driving enabling a larger δ [67,68]. Such techniques, when combined with achievable reductions in dephasing noise, could bring state preparation infidelities of the Gross and Ruskai codewords below QEC thresholds in the near term.

Outlook. We showed that global variational circuits of linear depth can prepare arbitrary superpositions of Dicke states. The circuit can be easily realized across a variety of experimental platforms. Its implementation could lead to the preparation of interesting and useful entangled states, with applications in quantum metrology and quantum error correction.

Finally, we note that the set of realizable interactions depends on the experimental platform, e.g., in cavity QED experiments dispersive interactions can be used to engineer the generator $\sin(J_z + \varphi)$ [25], whilst addressing the second red and blue sidebands in trapped ions can produce $\cosh(rJ_z) + \cos(\varphi)\sinh(rJ_z)$. These Hamiltonians can replace U_{OAT}; or the inclusion of more than one flavor of phase gate in the protocol could provide additional geometric control, potentially reducing the total number of gate steps required.

[1] D. Bluvstein, S. J. Evered, A. A. Geim, S. H. Li, H. Zhou, T. Manovitz, S. Ebadi, M. Cain, M. Kalinowski, D. Hangleiter, J. P. B. Ataides, N. Maskara, I. Cong, X. Gao, P. S. Rodriguez, T. Karolyshyn, G. Semeghini, M. J. Gullans, M. Greiner, V. Vuletić *et al.*, Logical quantum processor based on reconfigurable atom arrays, Nature (London) **626**, 58 (2023).

[2] S. Krinner, N. Lacroix, A. Remm, A. Di Paolo, E. Genois, C. Leroux, C. Hellings, S. Lazar, F. Swiadek, J. Herrmann, G. J. Norris, C. K. Andersen, M. Müller, A. Blais, C. Eichler, and A. Wallraff, Realizing repeated quantum error correction in a distance-three surface code, Nature (London) **605**, 669 (2022).

[3] V. V. Sivak, A. Eickbusch, B. Royer, S. Singh, I. Tsioutsios, S. Ganjam, A. Miano, B. L. Brock, A. Z. Ding, L. Frunzio, S. M. Girvin, R. J. Schoelkopf, and M. H. Devoret, Real-time quantum error correction beyond break-even, Nature (London) **616**, 50 (2023).

[4] B. M. Terhal, Quantum error correction for quantum memories, Rev. Mod. Phys. **87**, 307 (2015).

[5] Y. Ouyang, Permutation-invariant quantum codes, Phys. Rev. A **90**, 062317 (2014).

[6] M. B. Ruskai, Pauli exchange errors in quantum computation, Phys. Rev. Lett. **85**, 194 (2000).

[7] J. A. Gross, Designing codes around interactions: The case of a spin, Phys. Rev. Lett. **127**, 010504 (2021).

[8] G. Tóth, Multipartite entanglement and high-precision metrology, Phys. Rev. A **85**, 022322 (2012).

[9] Y. Ouyang and G. K. Brennen, Finite-round quantum error correction on symmetric quantum sensors, arXiv:2212.06285.

[10] M. Plesch and V. Bužek, Efficient compression of quantum information, Phys. Rev. A **81**, 032317 (2010).

[11] D. Bacon, I. L. Chuang, and A. W. Harrow, Efficient quantum circuits for schur and clebsch-gordan transforms, Phys. Rev. Lett. **97**, 170502 (2006).

[12] R. Prevedel, G. Cronenberg, M. S. Tame, M. Paternostro, P. Walther, M. S. Kim, and A. Zeilinger, Experimental realization of dicke states of up to six qubits for multiparty quantum networking, Phys. Rev. Lett. **103**, 020503 (2009).

[13] A. Bärtschi and S. Eidenbenz, Short-depth circuits for dicke state preparation, in *2022 IEEE International Conference on Quantum Computing and Engineering (QCE)* (2022), pp. 87–96.

[14] S. Aktar, A. Bärtschi, A.-H. A. Badawy, and S. Eidenbenz, A divide-and-conquer approach to dicke state preparation, Trans. Quantum Eng. **3**, 1 (2022).

[15] H. Buhrman, M. Folkertsma, B. Loff, and N. M. P. Neumann, State preparation by shallow circuits using feed forward, Quantum **8**, 1552 (2024).

[16] For example, the four $N = 3$ symmetric Dicke states are $|3/2, -3/2\rangle = |000\rangle$, $|3/2, -1/2\rangle = 1/\sqrt{3}(|001\rangle + |010\rangle + |100\rangle)$, $|3/2, 1/2\rangle = 1/\sqrt{3}(|011\rangle + |101\rangle + |110\rangle)$, and $|3/2, 3/2\rangle = |111\rangle$.

[17] H. J. Briegel and R. Raussendorf, Persistent entanglement in arrays of interacting particles, Phys. Rev. Lett. **86**, 910 (2001).

[18] X. Wang and K. Mølmer, Pairwise entanglement in symmetric multi-qubit systems, Eur. Phys, J. D. At. Mol. Opt. Phys. **18**, 385 (2002).

[19] J. K. Stockton, J. M. Geremia, A. C. Doherty, and H. Mabuchi, Characterizing the entanglement of symmetric many-particle spin- 1/2 systems, Phys. Rev. A **67**, 022112 (2003).

[20] A. Neven, J. Martin, and T. Bastin, Entanglement robustness against particle loss in multiqubit systems, Phys. Rev. A **98**, 062335 (2018).

[21] D. J. Wineland, J. J. Bollinger, W. M. Itano, and D. Heinzen, Squeezed atomic states and projection noise in spectroscopy, Phys. Rev. A **50**, 67 (1994).

[22] L. Pezzè, A. Smerzi, M. K. Oberthaler, R. Schmied, and P. Treutlein, Quantum metrology with nonclassical states of atomic ensembles, Rev. Mod. Phys. **90**, 035005 (2018).

[23] M. Koashi, V. Bužek, and N. Imoto, Entangled webs: Tight bound for symmetric sharing of entanglement, Phys. Rev. A **62**, 050302(R) (2000).

[24] W. Dür, G. Vidal, and J. I. Cirac, Three qubits can be entangled in two inequivalent ways, Phys. Rev. A **62**, 062314 (2000).

[25] M. T. Johnsson, N. R. Mukty, D. Burgarth, T. Volz, and G. K. Brennen, Geometric pathway to scalable quantum sensing, Phys. Rev. Lett. **125**, 190403 (2020).

[26] S. S. Ivanov, N. V. Vitanov, and N. V. Korolkova, Creation of arbitrary dicke and noon states of trapped-ion qubits by global addressing with composite pulses, New J. Phys. **15**, 023039 (2013).

[27] V. M. Stojanovic and J. K. Nauth, Dicke-state preparation through global transverse control of Ising-coupled qubits, Phys. Rev. A **108**, 012608 (2023).

[28] D. B. Hume, C. W. Chou, T. Rosenband, and D. J. Wineland, Preparation of dicke states in an ion chain, Phys. Rev. A **80**, 052302 (2009).

[29] C. Wu, C. Guo, Y. Wang, G. Wang, X.-L. Feng, and J.-L. Chen, Generation of dicke states in the ultrastrong-coupling regime of circuit qed systems, Phys. Rev. A **95**, 013845 (2017).

[30] K. D. B. Higgins, S. C. Benjamin, T. M. Stace, G. J. Milburn, B. W. Lovett, and E. M. Gauger, Superabsorption of light via quantum engineering, Nat. Commun. **5**, 4705 (2014).

[31] Y. Zhao, R. Zhang, W. Chen, X.-B. Wang, and J. Hu, Creation of Greenberger-Horne-Zeilinger states with thousands of atoms by entanglement amplification, npj Quantum Inf. **7**, 24 (2021).

[32] D. M. Greenberger, M. A. Horne, and A. Zeilinger, Going beyond bell's theorem, in *Bell's Theorem, Quantum Theory and Conceptions of the Universe*, edited by M. Kafatos (Springer Netherlands, Dordrecht, 1989), pp. 69–72.

[33] J. J. Bollinger, W. M. Itano, D. J. Wineland, and D. J. Heinzen, Optimal frequency measurements with maximally correlated states, Phys. Rev. A **54**, R4649(R) (1996).

[34] T. Monz, P. Schindler, J. T. Barreiro, M. Chwalla, D. Nigg, W. A. Coish, M. Harlander, W. Hänsel, M. Hennrich, and R. Blatt, 14-qubit entanglement: Creation and coherence, Phys. Rev. Lett. **106**, 130506 (2011).

[35] A. Omran, H. Levine, A. Keesling, G. Semeghini, T. T. Wang, S. Ebadi, H. Bernien, A. S. Zibrov, H. Pichler, S. Choi, J. Cui, M. Rossignolo, P. Rembold, S. Montangero, T. Calarco, M. Endres, M. Greiner, V. Vuletić, and M. D. Lukin, Generation and manipulation of schrödinger cat states in Rydberg atom arrays, Science **365**, 570 (2019).

[36] C. Song, K. Xu, H. Li, Y.-R. Zhang, X. Zhang, W. Liu, Q. Guo, Z. Wang, W. Ren, J. Hao, H. Feng, H. Fan, D. Zheng, D.-W. Wang, H. Wang, and S.-Y. Zhu, Generation of multicomponent atomic schrödinger cat states of up to 20 qubits, Science **365**, 574 (2019).

[37] E. Knill and R. Laflamme, A theory of quantum error-correcting codes, Phys. Rev. Lett. **84**, 2525 (2000).

[38] A. Bärtschi and S. Eidenbenz, Deterministic preparation of dicke states, in *Fundamentals of Computation Theory*, edited by L. A. Gasieniec, J. Jansson, and C. Levcopoulos (Springer International Publishing, Cham, 2019), pp. 126–139.

[39] X. Zou, K. Pahlke, and W. Mathis, Generation of arbitrary superpositions of the dicke states of excitons in optically driven quantum dots, Phys. Rev. A **68**, 034306 (2003).

[40] S. C. Carrasco, M. H. Goerz, Z. Li, S. Colombo, V. Vuletić, and V. S. Malinovsky, Extreme spin squeezing via optimized one-axis twisting and rotations, Phys. Rev. Appl. **17**, 064050 (2022).

[41] R. Kaubruegger, D. V. Vasilyev, M. Schulte, K. Hammerer, and P. Zoller, Quantum variational optimization of ramsey interferometry and atomic clocks, Phys. Rev. X **11**, 041045 (2021).

[42] R. Kaubruegger, P. Silvi, C. Kokail, R. Van Bijnen, A. M. Rey, J. Ye, A. M. Kaufman, and P. Zoller, Variational spin-squeezing algorithms on programmable quantum sensors, Phys. Rev. Lett. **123**, 260505 (2019).

[43] N. Gutman, A. Gorlach, O. Tziperman, R. Ruimy, and I. Kaminer, Universal control of symmetric states using spin squeezing, Phys. Rev. Lett. **132**, 153601 (2024).

[44] C. D. Marciniak, T. Feldker, I. Pogorelov, R. Kaubruegger, D. V. Vasilyev, R. Van Bijnen, P. Schindler, P. Zoller, R. Blatt, and T. Monz, Optimal metrology with programmable quantum sensors, Nature (London) **603**, 604 (2022).

[45] M. Kitagawa and M. Ueda, Squeezed spin states, Phys. Rev. A **47**, 5138 (1993).

[46] See Supplemental Material at http://link.aps.org/supplemental/10.1103/PhysRevResearch.7.L022072 for further analysis of potential sources of error in trapped ions, and details on the implementation of the protocol as a hybrid quantum-classical algorithm, which also includes Refs. [69–73].

[47] F. Albertini and D. D'Alessandro, Controllability of symmetric spin networks, J. Math. Phys. **59**, 052102 (2018).

[48] If there exists a control field $C(t)$ such that $\delta\mathcal{P}_{i \to f}/\delta C(t) = 0 \forall 0 \leqslant t \leqslant T$, where $\mathcal{P}_{i \to f} = |\langle\psi_f|U_{\text{tot}}|\psi_0\rangle|^2$ is the transition element for a transition from an initial (final) state $|\psi_0\rangle$ ($|\psi_f\rangle$) for some finite protocol time T, then the system is controllable.

[49] H. A. Rabitz, M. M. Hsieh, and C. M. Rosenthal, Quantum optimally controlled transition landscapes, Science **303**, 1998 (2004).

[50] J. Nocedal and S. J. Wright, *Numerical Optimization*, Springer Series in Operations Research and Financial Engineering (Springer New York, 2006).

[51] J. Bezanson, A. Edelman, S. Karpinski, and V. B. Shah, Julia: A fresh approach to numerical computing, SIAM Review **59**, 65 (2017).

[52] P. K. Mogensen and A. N. Riseth, Optim: A mathematical optimization package for Julia, J. Open Source Softw. **3**, 615 (2018).

[53] An offset c in the number of gates $P = \lceil 2N/3 \rceil + c$ is needed to reach fidelities below the numerical termination threshold $\epsilon = 10^{-12}$. For $N = 10$ to $N = 150$ the offset is either $c = 2$ or $c = 3$, depending on the ceil function. For $N = 200$ and $N = 250$ the offset is $c = 4$, to give the numerical optimization more overhead to reach the termination threshold. Specifically, for $N = [100, 150, 200, 250$ we use $P = [70, 103, 138, 171]$ gates.

[54] T. Keating, C. H. Baldwin, Y.-Y. Jau, J. Lee, G. W. Biedermann, and I. H. Deutsch, Arbitrary dicke-state control of symmetric Rydberg ensembles, Phys. Rev. Lett. **117**, 213601 (2016).

[55] D. C. Liu and J. Nocedal, On the limited memory BFGS method for large scale optimization, Math. Program. **45**, 503 (1989).

[56] I. Apellaniz, B. Lücke, J. Peise, C. Klempt, and G. Tóth, Detecting metrologically useful entanglement in the vicinity of dicke states, New J. Phys. **17**, 083027 (2015).

[57] Y. Ouyang, N. Shettell, and D. Markham, Robust quantum metrology with explicit symmetric states, IEEE Trans. Inf. Theory **68**, 1809 (2022).

[58] Note that the superposition of all states with only one qubit not excited $|N/2, N/2 - 1\rangle$ can be prepared using the same sequence by applying a global spin flip at the end of the sequence, and that optimizing for $|N/2, N/2 - 1\rangle$ rather than $|N/2, -N/2 + 1\rangle$ does not offer any potential for improvement as the initial state is an optimized CSS.

[59] P. W. Shor, Scheme for reducing decoherence in quantum computer memory, Phys. Rev. A **52**, R2493(R) (1995).

[60] K. Mølmer and A. Sørensen, Multiparticle entanglement of hot trapped ions, Phys. Rev. Lett. **82**, 1835 (1999).

[61] K. Kim, M.-S. Chang, R. Islam, S. Korenblit, L.-M. Duan, and C. Monroe, Entanglement and tunable spin-spin couplings between trapped ions using multiple transverse modes, Phys. Rev. Lett. **103**, 120502 (2009).

[62] J. Britton, B. C. Sawyer, C.-C. J. W. A. C. Keith, J. Freericks, H. Uys, M. J. Biercuk, and J. J. Bollinger, Engineered two-dimensional ising interactions in a trapped-ion quantum simulator with hundreds of spins, Nature (London) **484**, 489 (2012).

[63] J. Zhang, G. Pagano, P. W. Hess, A. Kyprianidis, P. Becker, H. Kaplan, A. V. Gorshkov, Z.-X. Gong, and C. Monroe, Observation of a many-body dynamical phase transition with a 53-qubit quantum simulator, Nature (London) **551**, 601 (2017).

[64] G. Kirchmair, J. Benhelm, F. Zähringer, R. Gerritsma, C. F. Roos, and R. Blatt, Deterministic entanglement of ions in thermal states of motion, New J. Phys. **11**, 023002 (2009).

[65] A. Sørensen and K. Mølmer, Entanglement and quantum computation with ions in thermal motion, Phys. Rev. A **62**, 022311 (2000).

[66] W. Ge, B. C. Sawyer, J. W. Britton, K. Jacobs, J. J. Bollinger, and M. Foss-Feig, Trapped ion quantum information processing with squeezed phonons, Phys. Rev. Lett. **122**, 030501 (2019).

[67] Y. Shapira, R. Shaniv, T. Manovitz, N. Akerman, L. Peleg, L. Gazit, R. Ozeri, and A. Stern, Theory of robust multiqubit nonadiabatic gates for trapped ions, Phys. Rev. A **101**, 032330 (2020).

[68] J. D. Arias Espinoza, K. Groenland, M. Mazzanti, K. Schoutens, and R. Gerritsma, High-fidelity method for a single-step n-bit toffoli gate in trapped ions, Phys. Rev. A **103**, 052437 (2021).

[69] L. Bond, L. Lenstra, R. Gerritsma, and A. Safavi-Naini, Effect of micromotion and local stress in quantum simulations with trapped ions in optical tweezers, Phys. Rev. A **106**, 042612 (2022).

[70] J. R. McClean, J. Romero, R. Babbush, and A. Aspuru-Guzik, The theory of variational hybrid quantum-classical algorithms, New J. Phys. **18**, 023023 (2016).

[71] A. Peruzzo, J. McClean, P. Shadbolt, M.-H. Yung, X.-Q. Zhou, P. J. Love, A. Aspuru-Guzik, and J. L. O'Brien, A variational eigenvalue solver on a photonic quantum processor, Nat. Commun. **5**, 4213 (2014).

[72] G. Tóth, W. Wieczorek, D. Gross, R. Krischek, C. Schwemmer, and H. Weinfurter, Permutationally invariant quantum tomography, Phys. Rev. Lett. **105**, 250403 (2010).

[73] G. Tóth, W. Wieczorek, R. Krischek, N. Kiesel, P. Michelberger, and H. Weinfurter, Practical methods for witnessing genuine multi-qubit entanglement in the vicinity of symmetric states, New J. Phys. **11**, 083002 (2009).